

A. SHUMELYUK<sup>1</sup>  
S. ODOULOV<sup>1,✉</sup>  
O. OLEYNIK<sup>1,2</sup>  
G. BROST<sup>3</sup>  
A. GRABAR<sup>4</sup>

# Spectral sensitivity of nominally undoped photorefractive Sn<sub>2</sub>P<sub>2</sub>S<sub>6</sub>

<sup>1</sup> Institute of Physics, National Academy of Sciences, Nauky av. 46, 03028 Kiev, Ukraine

<sup>2</sup> National O.O. Bogomoletz Medical University, 01004 Kiev, Ukraine

<sup>3</sup> Air Force Research Laboratory/SNRD, 26 Electronic Pkwy, Rome, NY 13441-4515, USA

<sup>4</sup> Institute of Solid State Physics and Chemistry, Uzhgorod State University, 88000 Uzhgorod, Ukraine

Received: 30 January 2007  
© Springer-Verlag 2007

**ABSTRACT** Nominally undoped tin hypthiodiphosphate is shown to possess photorefractive sensitivity from its band edge in the visible region of the spectrum up to 1.3 μm in the near infrared. The gain factor decreases with the increasing wavelength while the characteristic rate of photorefractive build-up roughly follows the spectral dependence of photoconductivity.

**PACS** 42.65.Hw; 42.70.Nq

## 1 Introduction

Tin hypthiodiphosphate (Sn<sub>2</sub>P<sub>2</sub>S<sub>6</sub>, SPS) is a ferroelectric crystal with  $P_c$  symmetry at room temperature and bandgap at  $E_g = 2.3$  eV [1, 2]. Photorefractive recording [3] has been reported in this material at  $\lambda = 0.63$  μm [4, 5] and at  $\lambda = 1.064$  μm (with pre-exposure to white light) [6, 7]. Charge hopping was shown to be the reason for the space charge formation in the near infrared region [6]. In nominally undoped crystals the gain factor at  $\lambda = 1.06$  μm is  $7$  cm<sup>-1</sup>. A gain factor up to  $16$  cm<sup>-1</sup> at  $\lambda = 1.06$  μm was reported for a “brown” modified crystal with unknown impurity [8]. However, according to our data the deliberately introduced impurities not always enhance the photorefractive response in the infrared. Dopants such as Fe, Se, Pb inhibit the photorefractive response at 1.06 μm even if sensitivity to the red light is slightly improved.

A gain factor  $\Gamma \geq 7$  cm<sup>-1</sup> is sufficient to build the photorefractive coherent oscillators that serve as self pumped phase conjugate mirrors [9]. Especially good performance, with phase conjugate reflectivity up to 90%, ensure Te doped and “brown” modified SPS in ring-loop cavity [10, 11]. The advantage of nominally undoped material is, however, in their smaller absorption, especially near the band edge, which allows a broader wavelength response range with only one sample.

The purpose of this paper is to investigate the photorefractive response of nominally undoped material in the spectral interval where SPS crystals are transparent.

## 2 Absorption and photoconductivity

The SPS crystals were grown in Institute of Solid State Physics and Chemistry of Uzhgorod State University. The samples #2 and #3 (as mentioned in [5]) measure  $5 \times 5 \times 1.2$  mm<sup>3</sup>, and  $5 \times 9 \times 4.5$  mm<sup>3</sup>, respectively, the shortest face along OZ axis<sup>1</sup>. The axis of spontaneous polarization (OX axis) is nearly parallel to the input/output faces of the sample.

Figure 1 shows the measured spectra of optical absorption and photoconductivity for the light beam propagating along OY axis and polarized parallel to OX axis, electric current is measured along OX axis. The crystal is transparent for wavelengths greater than 0.55 μm. Starting from  $\lambda = 0.7$  μm, the absorption constant becomes less than  $1$  cm<sup>-1</sup>; for longer wavelengths it is not clear to what extent the measured extinction can be attributed to the absorption and what is due to the light scattering from the optical imperfections of the sample. In the photoconductivity spectrum one can see nearly exponential dependence on quantum energy  $\hbar\omega$ ,  $\sigma \propto \exp(\hbar\omega/\Delta E)$  with characteristic exponent  $\Delta E \approx 0.26 \pm 0.01$  eV.

## 3 Photorefractive response

To measure the standard two-beam coupling gain factor the dynamics of photorefractive grating is studied. Two coherent light waves impinge upon the sample in a plane parallel to the axis of spontaneous polarization (OX) and normal to input face. Both waves are identically polarized with the electric field vector in the plane of incidence. The intensity ratio of the weak signal wave to the strong pump wave is chosen to be close to 1 : 1000.

Four different laser sources were used to cover the range from 0.63 μm to 1.3 μm. These are He-Ne laser (0.63 μm), Ti:sapphire tunable laser (0.75–0.9 μm), diode-pumped Nd<sup>3+</sup>:YAG laser (1.064 μm), and diode-pumped Nd<sup>3+</sup>:YAG laser (1.3 μm). All these lasers have different output powers and different output beam cross sections but they all produce a single-mode, single-frequency cw output and

<sup>1</sup> We adopt and use the following notations for crystal axes: axis OY is normal to the mirror plane of the crystal, axis OX is nearly parallel to the axis of spontaneous polarization.

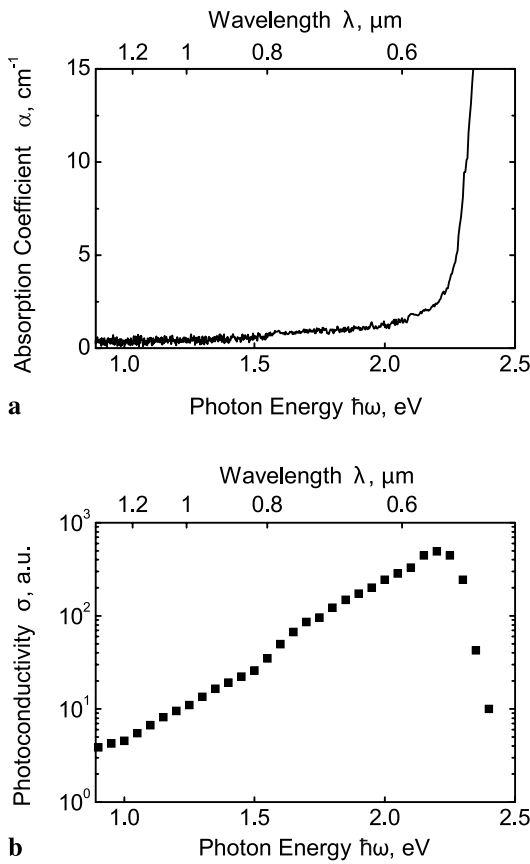


FIGURE 1 Absorption (a) and photoconductivity (b) spectra of  $\text{Sn}_2\text{P}_2\text{S}_6$

therefore ensure a large coherence length (except He-Ne laser with several longitudinal  $\text{TEM}_{00}$  modes oscillating simultaneously).

The dynamics of the beam-coupling in SPS is typical for photorefractive materials with two types of movable charge carriers (see, e.g., [12]). An example of temporal variation of the intensity of a weak beam is shown in Fig. 2. This particular graph relates to  $\lambda = 1.06 \mu\text{m}$ , but similar behavior is observed also at other wavelengths. When the pump wave is unblocked the intensity of the signal wave increases rapidly until a certain peak value is reached. After that, the intensity of the amplified wave decreases slowly and finally comes to

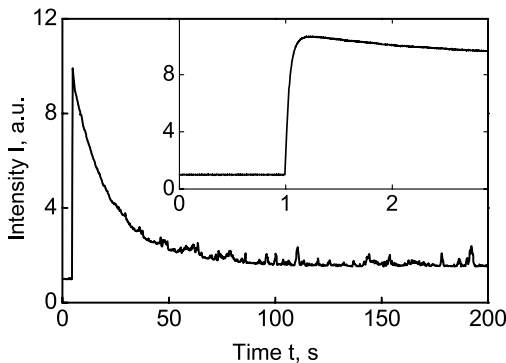


FIGURE 2 Dynamics of weak beam intensity in beam-coupling experiment with  $\lambda = 1.06 \mu\text{m}$ ; inset shows the initial stage of recording with enlarged scale

a steady state which is much smaller than the peak value. It has been shown that the slow decay is caused by presence in SPS of thermally excited carriers [6, 13]. This decay can be eliminated by cooling of the sample to  $-30$  to  $-50 \text{ }^\circ\text{C}$  or by the use of a moving grating technique [8]. Because of the considerable difference in characteristic decay time for the fast and slow gratings the peak value of the gain factor practically coincides with the steady state gain for the fast grating only. This was proven both experimentally [13] and theoretically [14]. In the present study we concentrate on measurements of the gain for the transient peak. The gain factor,  $\Gamma = (1/d) \ln(I_{\text{peak}}/I_0)$ , is measured, with  $I_{\text{peak}}$  and  $I_0$  standing for maximum peak intensity and initial transmitted through the sample intensity (with no pump beam), respectively, and sample thickness  $d$ .

It has been reported in [6] that the sensitivity of the sample to the recording in the near infrared region of the spectrum can be increased by pre-illumination of the sample with visible light. Once illuminated, the sample remains sensitive for several days. To ensure the same conditions for recording at any studied wavelength we illuminated the sample every morning for 5 min with light from of halogen lamp (100 W) placed 5 cm-away from the sample.

We first measured the grating spacing dependencies of gain factor for different wavelengths. Figure 3 illustrates such a dependence for  $\lambda = 0.75 \mu\text{m}$ . The maximum gain factor is reached at  $\Lambda = 0.75 \mu\text{m}$ . The similar dependence for  $\lambda = 1.06 \mu\text{m}$  revealed the maximum at  $\Lambda$  slightly less than  $1 \mu\text{m}$ . This shift in the gain factor dependence on grating spacing reflects a wavelength dependence of the Debye screening length. Apparently, at shorter wavelengths free carriers are excited from additional donor centers, thus increasing the effective trap density.

Next we measured the intensity dependencies of the gain factor for different wavelengths. The results are summarized in Fig. 4. Three curves are shown, for  $\lambda = 0.63, 0.75 \mu\text{m}$  and  $\lambda = 1.06 \mu\text{m}$ . Only one point is shown for  $\lambda = 1.3 \mu\text{m}$  at high intensity, due to poor signal to noise ratio at lower intensities. The pronounced intensity dependencies are evident. A greater intensity is needed at longer wavelengths to obtain the same gain factor that is achieved at shorter wavelengths.

Lastly, we measured the wavelength dependence of the gain factor with the same intensity of the pump wave ( $I = 0.8 \text{ W/cm}^2$ ) and the same crossing angle between the two writing waves ( $2\theta = 60^\circ$ ). The results are shown in Fig. 5a. The gain factor decreases with increasing wavelength. This

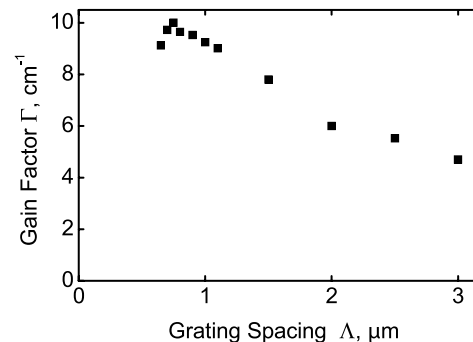
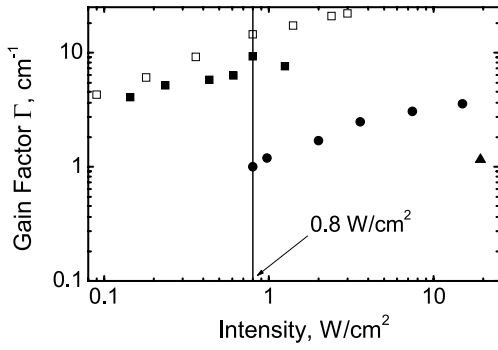
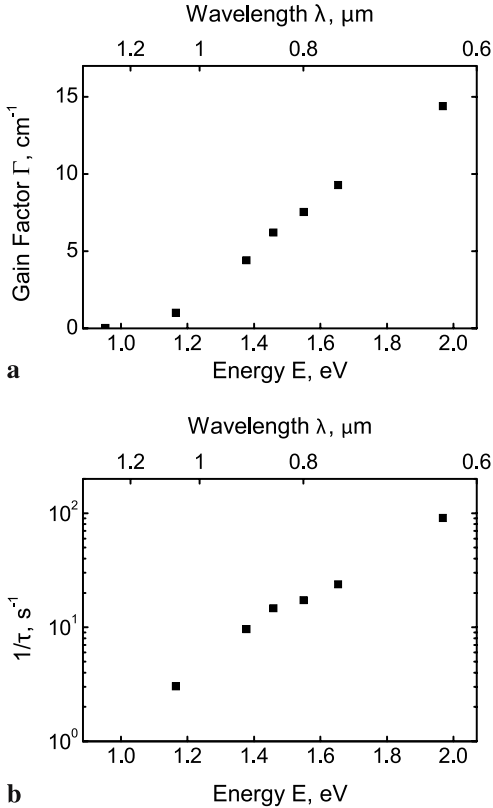


FIGURE 3 Gain factor versus grating period for  $\lambda = 0.75 \mu\text{m}$ ;  $I = 1.25 \text{ W/cm}^2$



**FIGURE 4** Intensity dependence of gain factor for  $\lambda = 0.63 \mu\text{m}$  (open box),  $0.75 \mu\text{m}$  (filled box),  $1.06 \mu\text{m}$  (filled circles), and  $1.3 \mu\text{m}$  (filled triangle)



**FIGURE 5** Wavelength dependence of the gain factor (a) and grating build-up time (b) for  $I = 0.8 \text{ W/cm}^2$  and  $2\theta = 60^\circ$

is explained in part by the decrease of the diffusion field  $E_D$  for a selected angle  $2\theta$  between the recording waves. With  $E_D = (0.163/\Lambda) \text{ V/cm}$  and  $\Lambda$  measured in cm one can expect at room temperature a 36% decrease of the gain factor when increasing the wavelength from  $0.63 \mu\text{m}$  to  $1 \mu\text{m}$ . In fact, we observe an order of magnitude decrease of the gain factor in the same wavelength range, which must be attributed to other reasons.

The decrease in photoconductivity leads to a longer relaxation time for the “fast” grating component. We observe an increase of the rise time (time needed to reach the peak value of gain) from 11 ms at  $\lambda = 0.63 \mu\text{m}$  to 330 ms at  $\lambda = 1.064 \mu\text{m}$  for the same intensity  $I = 0.8 \text{ W/cm}^2$  (Fig. 5b). According to the standard model of photorefraction, the grating relaxation time  $\tau$  should be proportional to dielectric relaxation time  $\tau_{\text{di}}$  and to correction factors that depend on grating spacing; De-

bye screening length  $l_s$  and diffusion length  $l_D$  [11]. As  $\tau_{\text{di}} = \epsilon\epsilon_0/\sigma$  one can expect that the build-up rate (the reciprocal relaxation time  $\tau^{-1}$ ) will increase with the quantum energy in similar way as conductivity does, i.e.,  $(1/\tau) \propto \exp(\hbar\omega/\Delta E)$ . The value  $\Delta E \approx (0.24 \pm 0.02) \text{ eV}$  estimated from the data of Fig. 5b is in good agreement with  $\Delta E \approx (0.26 \pm 0.01) \text{ eV}$  evaluated from the photoconductivity spectrum (Fig. 1b).

#### 4 Discussion and conclusions

We presented in this paper a comparative data on the amplitude and characteristic time of photorefractive response of SPS crystals in the spectral region from  $0.63 \mu\text{m}$  and  $1.3 \mu\text{m}$ , where the crystal is transparent and still sensitive. As both quantities ( $\Gamma$  and  $\tau$ ) are functions of several wavelength dependent parameters, a comparison of data for different wavelengths is always problematic and consequently the graphs shown here represent the general tendency of the spectral dependencies.

One possible way of comparison is to keep constant a certain diffusion field and measure the wavelength dependence of the gain factor. The obvious disadvantage of this technique is in necessity to readjust the intersection angle for any new wavelength. Another difficulty comes from the wavelength dependence of the Debye screening length  $l_s$ . By changing the wavelength, we excite free carriers from other donor centers which changes the effective trap density. This results in modification of space-charge screening and in a shift of gain factor maximum in the dependence on grating spacing and, therefore, modifies the spectral dependence.

We impose in our measurements the constant crossing angle  $2\theta = 60^\circ$ , i.e., the fringe spacing  $\Lambda = \lambda$  for any particular wavelength. Within the measured spectral interval a condition  $\Lambda \approx \lambda$  ensured the values of gain factor close to the maximum, reached at  $\Lambda = 2\pi l_s$ . This ensures that values of gain factor close to that optimized for fringe spacing are compared. With this evaluation technique, we conclude that for the recording intensity  $I = 0.8 \text{ W/cm}^2$  one can reach 14 times larger value of  $\Gamma$  (and 30 time smaller value of  $\tau$ ) at  $0.63 \mu\text{m}$  as compared to  $\Gamma$  and  $\tau$  at  $1.06 \mu\text{m}$ . One needs to keep in mind that unusual intensity dependence of photorefractive response in SPS [5] allows one to reach rather large values of gain in the infrared for more powerful light beams. Thus, Tin hypotiodiphosphate can be successfully used for wave-mixing experiments in over the whole spectral range covered by Ti-sapphire and  $\text{Nd}^{3+}:\text{YAG}$  lasers.

**ACKNOWLEDGEMENTS** We are grateful to Kevin Magde for his contribution in the initial stage of this work, to Dean Evans and Gary Cook for helpful discussion. Financial support of Science and Technology Center and European Office of Research and Development (Project P232) is gratefully acknowledged.

#### REFERENCES

- 1 C.D. Carpentier, R. Nitsche, Mater. Res. Bull. **9**, 401 (1974)
- 2 G. Dittmar, H. Schaefer, Z. Naturforsch. **29b**, 312 (1974)
- 3 A. Grabar, Y. Vysochanskii, A. Shumelyuk, M. Jazbinek, G. Montemazzani, P. Gunter, Springer Ser. in Optical Sciences Vol. 114 (2006)
- 4 A.A. Grabar, R.I. Muzhikash, A.D. Kostjuk, Y.M. Vysochanskii, Sov. Phys. Solid State **33**, 1314 (1991)

- 5 A. Shumelyuk, D. Barilov, S. Odoulov, E. Krätzig, *Appl. Phys. B* **76**, 417 (2003)
- 6 S.G. Odoulov, A.N. Shumelyuk, U. Hellwig, R.A. Rupp, A.A. Grabar, I.M. Stoyka, *J. Opt. Soc. Am. B* **13**, 2352 (1996)
- 7 M. Weber, G. von Bally, A. Shumelyuk, S. Odoulov, *Appl. Phys. B* **74**, 29 (2002)
- 8 A.A. Grabar, I.V. Kedyk, M.I. Gurzan, I.M. Stoika, A.A. Molnar, Y.M. Vysochanskii, *Opt. Commun.* **188**, 187 (2001)
- 9 A. Shumelyuk, S. Odoulov, G. Brost, *Appl. Phys. B* **68**, 956 (1999)
- 10 M. Jazbinšek, D. Haertle, G. Montemezzani, P. Günter, A.A. Grabar, I.M. Stoika, Y.M. Vysochanskii, *J. Opt. Soc. Am. B* **22**, 2459 (2005)
- 11 T. Bach, M. Jazbinšek, P. Günter, A. Grabar, I. Stoika, Y. Vysochanski, *Opt. Express* **13**, 9890 (2005)
- 12 S. Zhivkova, M. Miteva, *J. Appl. Phys.* **68**, 3099 (1990)
- 13 S. Odoulov, A. Shumelyuk, G. Brost, K. Magde, *Appl. Phys. Lett.* **69**, 3665 (1996)
- 14 A. Shumelyuk, S. Odoulov, G. Brost, *J. Opt. Soc. Am. B* **15**, 2125 (1998)